Journal of Digital Imaging (2018) 31:553–561
https://doi.org/10.1007/s10278-017-0040-0

A Novel Method for Correcting Non-uniform/Poor Illumination of Color Fundus Photographs

Sajib Kumar Saha[1] · Di Xiao[1] · Yogesan Kanagasingam[1]

Published online: 5 December 2017

Abstract
Retinal fundus images are often corrupted by non-uniform and/or poor illumination that occur due to overall imperfections in the image acquisition process. This unwanted variation in brightness limits the pathological information that can be gained from the image. Studies have shown that poor illumination can impede human grading in about 10~15% of retinal images. For automated grading, the effect can be even higher. In this perspective, we propose a novel method for illumination correction in the context of retinal imaging. The method splits the color image into luminosity and chroma (i.e., color) components and performs illumination correction in the luminosity channel based on a novel background estimation technique. Extensive subjective and objective experiments were conducted on publicly available DIARETDB1 and EyePACS images to justify the performance of the proposed method. The subjective experiment has confirmed that the proposed method does not create false color/artifacts and at the same time performs better than the traditional method in 84 out of 89 cases. The objective experiment shows an accuracy improvement of 4% in automated disease grading when illumination correction is performed by the proposed method than the traditional method.

Keywords Color fundus image · Illumination correction · Automated pathology detection · Deep learning

Introduction

Fundus photography is a widely used imaging modality for non-invasive examination of the eye and is considered an efficient modality to screen for and diagnose several eye diseases including age-related macular degeneration (AMD) [1] and diabetic retinopathy (DR) [2]. The widespread availability of fundus cameras and the easily manageable data format have made this imaging popular nowadays [3, 4].

Retinal images obtained in a screening program are acquired at different sites, using different cameras that are operated by qualified people who have varying levels of experience [4]. Fundus images frequently show unwanted variations in brightness due to overall imperfections in the imaging instrument itself [5–7] or by error in the alignment of the measurement subject [7]. Figure 1 shows a typical example of non-uniform illumination in fundus image in which the center of the image is considerably brighter than its surroundings.

This non-uniformness in illumination across the retina limits the pathological information that can be gained from the image. Studies have shown that poor illumination can impede human grading in about 10~15% of retinal images [8]. For automated grading, non-uniform and/or poor illumination can significantly affect the grading performance [9, 10]. Thus, methods for automated correction of non-uniform/poor illumination have got utmost importance. Majority of the illumination correction methods in retinal imaging context focuses on gray scale or green channel of the RGB fundus image [11, 12]. Green channel is typically considered more robust against noise compared to other channels in RGB fundus image and is used explicitly for automated detection and analysis of pathologies. Thus, performing illumination correction only on the green channel serves the purpose to some extent. However, the use of color information for detection/ analysis of pathologies is very likely to bring further improvement, especially when we already know that color serves as an important visual clue among different pathologies [13, 14] in fundus photographs. On that perspective, this paper focuses on developing illumination correction methods for color fundus images.

✉ Sajib Kumar Saha
Sajib.Saha@csiro.au

[1] Australian e-Health Research Centre, Commonwealth Scientific and Industrial Research Organisation, Perth, Australia

Fig. 1 An example fundus image which shows poor/ non-uniform illumination

In recent years, a few arbitrary attempts are made to develop illumination correction methods for color fundus photographs [9, 15, 16]. While these methods were found to improve the automated detection/classification accuracy of certain pathologies [9], or to improve the segmentation of retinal vessels [16], it remained unjustified whether these methods will create false color/artifacts on the image or not. Unsurprisingly, creation of false color/ artifacts is very likely to interfere with other pathology detection/classification.

In this paper, we propose an illumination correction method of color fundus photograph that does not create false color/ artifacts in the image, which we validate through extensive subjective experiment. The simple and efficient background subtraction based illumination correction method [17] has been amended by incorporating a novel background estimation technique and by adapting the model for color image processing.

Specific contributions of the paper include:

1. A novel method for illumination correction of color fundus photographs. Specifically, we augment the background subtraction based illumination correction model for color image processing and propose a novel background estimation technique in the context of retinal imaging.
2. Extensive subjective experiment to justify that the proposed method does not create false artifacts at least in the areas that did not suffer non-uniform or poor illumination prior to correction.
3. Subjective and objective experiments to justify that the proposed method performs better than the traditional method.

Related Works

Several methods for non-uniform illumination and shade correction have been described in the literature. Popular methods for non-uniform illumination and shade correction can be classified into filtering-based [18, 19], surface fitting-based [20], segmentation-based [21], and others. Filtering-based methods assume that shading components that have distorted the image can be estimated by filtering the acquired image with a low-pass filter. Surface fitting method assumes that the intensity variations of the background can be estimated by fitting a shading model [22]. Usually, a second-order polynomial is used as the function of the model for least-squares fitting. Segmentation-based method repeatedly performs image segmentation and bias field fitting [21]. Histogram equalization [17], Gamut mapping and Gamma correction [23], and Retinex approach [24, 25] are some of the other commonly used methods for illumination correction. Each of the methods has its pros and cons [15]. This paper focuses on filtering-based methods which are typically considered simple, however, efficient [16].

Specific methods for illumination corrections have been already proposed for retinal image processing and analysis. Simple and fast method using large-kernel median filter to obtain a low-pass correction coefficients in retinal images was proposed by Niemann in [26]. Narasimha-Iyeret et al. [27] proposed an illumination correction method that combines the advantages of filtering and surface fitting. The method also exploits and uses retina-specific information. In [10], Foracchia et al. proposed a method for automated luminosity and contrast normalization of retinal images. The method estimates of the luminosity and contrast variability in the background part of the image and then develops methods to compensate them. Leahy et al. [7] applied Laplace interpolation and a multiplicative image formation model illumination correction of retinal images. In [28], Zheng et al. used the sparsity property of image gradient distribution for illumination correction of retinal fundus images. Majority of the illumination correction methods in retinal image analysis uses only the green channel of the RGB photograph. There are only a few methods that perform illumination correction of color fundus images. In an attempt to perform illumination correction of the color fundus photographs, Grisan et al. proposed a model-based approach in [15]. The method uses the hue, saturation, and value (HSV) color space to better decouple the luminance and chromatic information. Then, it fits an illumination model on a proper subregion (the retinal background) of the saturation and value channels. Kolar et al. [16] relied on B-spline approximation of the illumination surface to perform illumination correction. Varnousfaderani et al. [9] used LUV color space transformation and a standard reference image for illumination correction as well as contrast enhancements. These methods in general does not justify whether they will create false color/artifacts on the image or not. We differ from these studies by providing a clear justification through our subjective experiment that shows the proposed method does not create false color/artifacts at least on the areas that did not suffer non-uniform/poor illumination prior to correction. At the same time, we have performed extensive subjective and objective experiments to vindicate that the proposed method performs better than the traditional method.

Proposed Illumination Correction

Color Transform to Split the Luminance Channel

RGB color space is not well suited for illumination correction and chromatic preservation, since the channels are correlated [15]. Therefore, color space transformation is required to transform the RGB image into a space where luminosity can be separated from the chroma. Widely used color transformation models include HSV [15, 29], LUV [9, 29], and LAB [29]. Inspired by the findings of Grisan et al. [15], we have used HSV color space transform [30] here. HSV color space contains three components—hue, saturation, and value [30, 31], where the value channel represents the luminance. HSV components are computed from the RGB values as below:

$$R' = \frac{R}{255},\quad G' = \frac{G}{255},\quad B' = \frac{B}{255}.$$

$$C_{\max} = \max\left(R', G', B'\right).$$

$$C_{\min} = \min\left(R', G', B'\right).$$

$$\Delta = C_{\max} - C_{\min}.$$

$$\text{Hue},\quad H = \begin{cases} 60^o \times \left(\frac{G'-B'}{\Delta} \mod 6\right) & if\ \ C_{\max} = R' \\ 60^o \times \left(\frac{B'-R'}{\Delta} + 2\right) & if\ \ C_{\max} = G' \\ 60^o \times \left(\frac{R'-G'}{\Delta} + 4\right) & if\ \ C_{\max} = B' \end{cases};$$

$$Saturation,\quad S = \begin{cases} 0 & if\ \ C_{\max} = 0 \\ \frac{\Delta}{C_{\max}} & else \end{cases};$$

$$Value,\quad V = C_{\max}.$$

Background Estimation and Illumination Correction

The illumination correction system we propose is based on the following background subtraction model [32]

$$f' = f - b + mean\ \ (b),$$

where f is the observed image, b is the background image, mean (b) represents the mean of the background image, and $\acute{f}$ is the image after correction.

Typically, the background is estimated by applying a smoothing filter (e.g., median filter [26], Gaussian filter [17]) with a very large kernel on the original image [16]. The major drawback of this method is that it may cause smoothing effect on pathological regions [15]. This may lead to poor pathological detection. Here, we proposed a novel background estimation method that overcomes this problem.

To estimate the background image, we rely on the following model of the observed fundus image f:

$$f = g(f^o) = g\left(f^o_{back} + f^o_{foreground}\right),$$

where f^o is the original image, f^o_{back} is the original background image, and $f^o_{foreground}$ is the original foreground image.

The original background image f^o_{back} is free of any vascular structure, optic disk, and visible lesions. The original foreground image $f^o_{foreground}$ on the other hand includes vascular structures, the optic disk, visible pathology, etc., i.e., all the features that are not in the background image.

To compute the background image, we require a preliminary extraction of the pixels belonging to the background set β. To form β, we rely on the following two assumptions about the background pixels [10]:

1. The intensity values of background and foreground pixels are different enough to be detected.
2. In a neighborhood of $w \times w$ pixels, at least 50% of them are background pixels.

The window size $w \times w$ plays an important role for the assumptions to be satisfied. Ideally, the window size should be big enough so that when it covers the biggest pathology in the image, at least 50% pixels in the window are still background. However, bigger window size causes computational cost to increase significantly. In this work, experimentally, we found that w equal to one-half of the optic disk diameter provides an optimal choice. It is worth mentioning when the above assumptions are not satisfied, for example, for extremely large pathology (in a part of the image), then the background image generated (for that part of the image) by the proposed method and the traditional method will be identical; which eventually means in the worst-case scenario as well, the proposed method will perform at least as good as the traditional method.

To implement the above assumptions what is done is for each pixel (x, y) in the image, we compute a mean intensity $\mu(x, y)$ using a window of size $w \times w$ around the (x, y), which is then compared with the pixel's intensity. The pixel (x, y) belongs to β if its intensity is close to the mean intensity. This is mathematically expressed by saying that the pixel (x, y) belongs to β if $|\mu(x, y) - f(x, y)| < t$, where $f(x, y)$ is the intensity of the pixel (x, y) and t is a predefined threshold. The value of t has been experimentally set to 0.015.

The background image b is computed by applying a Gaussian blur of σ, equal to one half of w on β.

Figure 2 shows the luminosity channel of the image shown in Fig. 1, pixels belonging to the background set, and the luminosity image obtained after illumination correction.

Efficient Computation of Mean Intensity

The proposed approach requires computing the mean intensity within a window for each pixel of the image. To ensure efficient computation, integral image [33, 34] is used. Integral image is an efficient way of computing sum of values of rectangular subset within an image. It is a two-dimensional array, and the value at a point (x, y) in the array is just the sum of all the elements above and to the left of (x, y). Mathematically, the integral image $f_{\sum}$ is computed from the original image f as below,

$$f_{\sum} = \sum_{y' \le y}^{x' \le x} f\left(x', y'\right).$$

Once we have computed $f_{\sum}$, then the summation of intensities within a window $w \times w$ around (x, y) is computed as below,

$$s(x,y) = f_{\sum}\left(x + \frac{w}{2}, y + \frac{w}{2}\right) + f_{\sum}\left(x - \frac{w}{2}, y - \frac{w}{2}\right) - f_{\sum}\left(x - \frac{w}{2}, y\right) - f_{\sum}\left(x, y - \frac{w}{2}\right).$$

From $s(x, y)$, the mean $\mu(x, y)$ is computed as below,

$$\mu(x,y) = \frac{s(x,y)}{w \times w}.$$

Experimental Analysis

Subjective Experiment

Subjective experiment was conducted to visually analyze the effect of illumination correction methods on the appearances of pathologies in the images. The experiment was performed in the presence of an experienced ophthalmologist. The proposed method, the traditional method, and the original image prior to corrections were compared. In order to have a fair comparison, Gaussian smoothing and HSV color space transformation were used for the traditional method as well.

Figure 3 shows an example color fundus image with poor and non-uniform illumination, the corrected image by the proposed method, and the image produced by traditional method.

Dataset

The publicly available DIARETDB1 dataset (http://www.it.lut.fi/project/imageret/diaretdb1/) was used for the experiment. The dataset contains 89 color fundus images of dimensionality 1500×1152. The visible pathologies that are present in the images include microaneurysms, hemorrhages, and soft and hard exudates. The pathologies were outlined by four independent experts. The images were either optic disc (OD) or macula-centered.

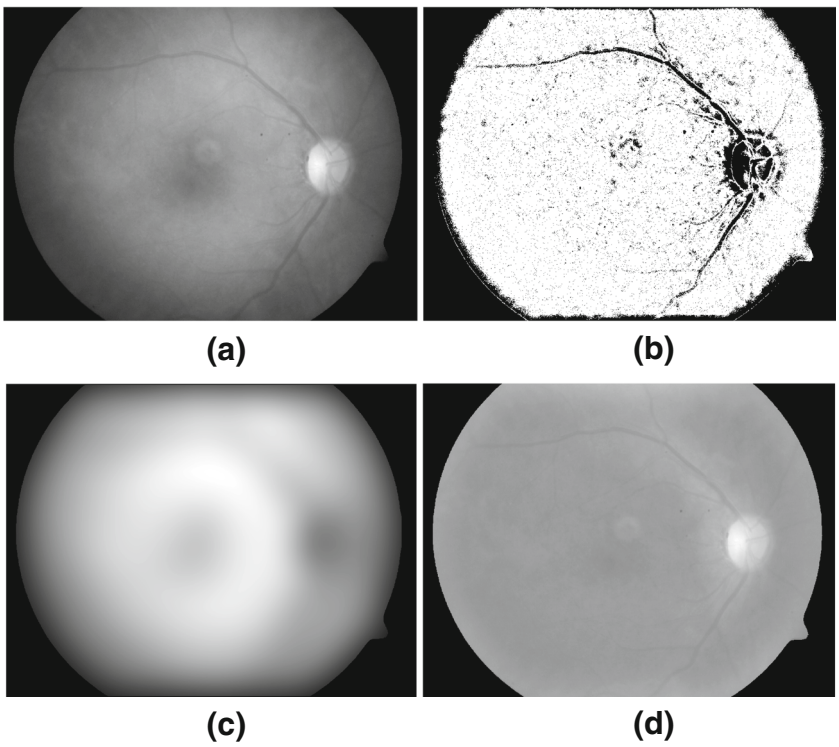

Fig. 2 Background estimation and illumination correction on an example image. **a** Luminosity channel of the image shown in Fig. 1. **b** Background and foreground pixels following intensity thresholding—1 means foreground and 0 means background. **c** Estimated background by the proposed method. **d** Illumination-corrected luminosity channel

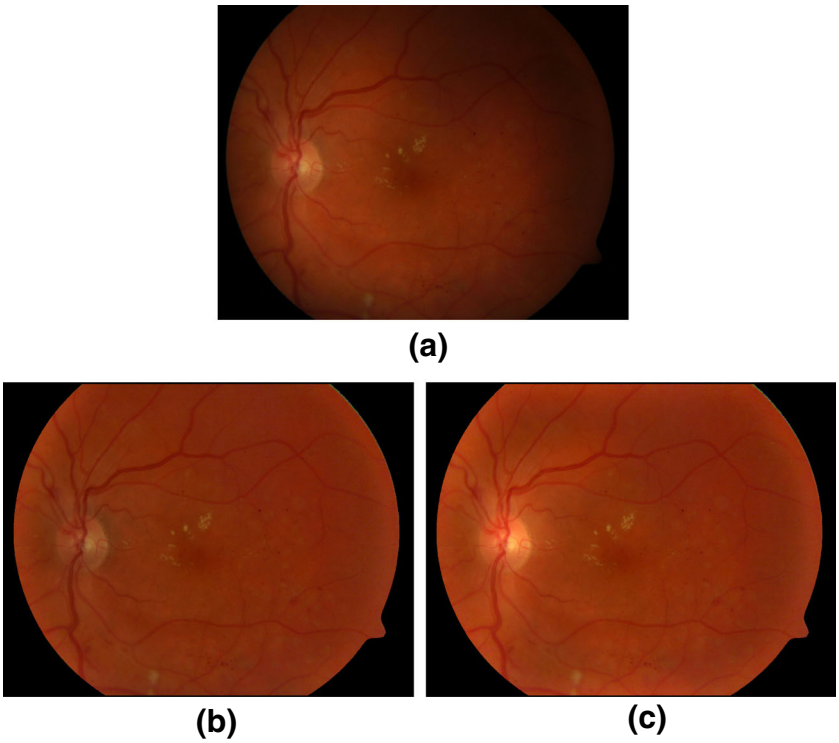

Fig. 3 An example of fundus images before and after illumination correction. **a** Example image with non-uniform illumination. **b** Corrected image by the traditional method. **c** Corrected image by the proposed method

Experiments and Results

One experienced ophthalmologist performed the experiment. A computer platform was developed for the experiment. Three different images including the original image, the image produced by the proposed correction method, and the image produced by the traditional method were shown on the platform. The ophthalmologist was asked to rank the images based on how clinically informative they were, specifically, based on visibility of pathologies, overall color appearance, illumination, and contrast. While choosing a processed image over the original, the ophthalmologist was told to be careful that the processed image should not create false color or artifacts at least in the regions that were clearly visible in the original image. At the same time, the ophthalmologist should choose the original image as the best if he found any pathologies that were visible in the original image, however, became dimmed in the processed image. The ophthalmologist had the option to give comments for any particular selection.

A snapshot of the platform is shown in Fig. 4.

It is worth mentioning, in order to avoid any possible bias, the ophthalmologist was not made aware that method 1 (Fig. 4) corresponds to the proposed method and method 2 corresponds to the traditional approach.

Figure 5 depicts the findings of the experiment.

From the illustration, it is observable that in majority of the cases, the ophthalmologist chose the corrected images over the original images, 84 out of 89 cases to be exact. Out of these 84 cases, in 80 cases, the corrected images produced by the proposed method were ranked better than the corresponding one from the traditional method. The ophthalmologist chose the original images over the corrected images in 5 out of 89 cases. By analyzing the image data and ophthalmologist's comments, we found that in 1 out these 5 cases, the original images had a barely noticeable non-uniformness in illumination and, at the same time, the processed methods did not make them look any better. In the rest 4 cases, illumination correction methods affected the visibility of the pathologies (pathologies appeared dim) to some extent (though slightly). Of these 5 cases, in 4 cases the proposed method was ranked topper than the traditional method. Overall, neither the proposed nor the traditional method was found to produce false color/artifacts on the images to an extent that would be relevant in practice; however, the tradition method was found to make the pathologies to appear dim in many cases.

Objective Experiment

Here, computer vision methods were applied for automated pathology detection/classification and grading of the images prior and after illumination correction. Color fundus images obtained from DIARETDB1 and Kaggle (https://www.kaggle.com/c/diabetic-retinopathy-detection/data) datasets were used for the experiment.

In the first part of the experiment, we applied a machine leaning technique to detect and classify DR pathologies, namely, microaneurysms, hard exudates, soft exudates, and hemorrhages. DIARETDB1 dataset had 89 images—28

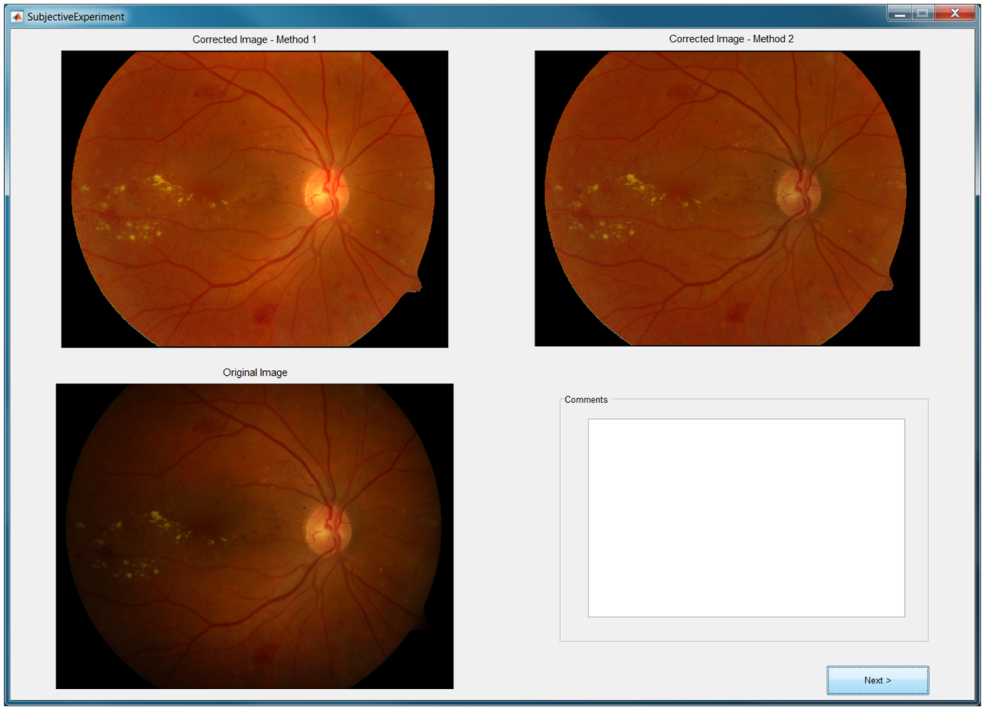

Fig. 4 A snapshot of the computer platform

training images and 61 test images. The ground truth images representing the pathologies of these images were also available.

We applied the deep learning framework proposed in [35] for the automated detection and classification of pathologies from the images. Deep features of dimensionality 4096 were learnt at the first fully connected layer. Support vector machine (SVM) classifier was applied on top of these activation features to classify the pathologies. LibSVM (https://www.csie.ntu.edu.tw/~cjlin/libsvm/) toolbox was used with default parameters. Optic disk (OD) [36] detection was also performed prior to deep learning to avoid the ambiguous color feature match with exudates.

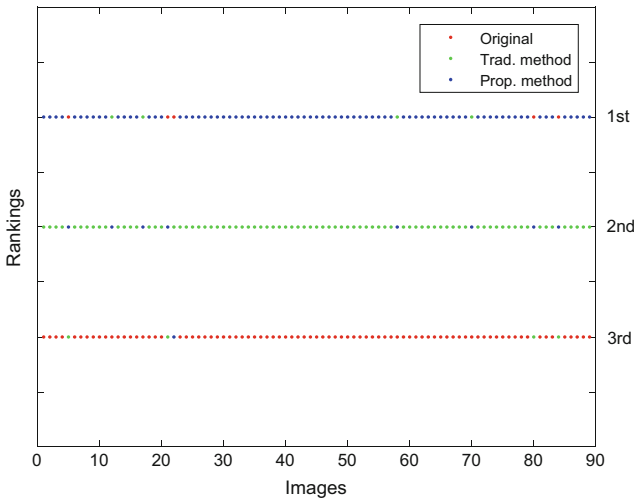

Fig. 5 Ranking of images by the participant. Each dot represents an image

Figure 6 shows the receiver operating characteristic (ROC) curves for the detection and classification of DR features. Table 1 summarizes the area under the ROC curves obtained for different methods.

From the results, it is observable that microaneurysms are likely to be better detected/classified on the processed images than on the original images. However, for other pathologies, improvements are not to an extent that would be relevant in practice. The difference between the proposed method and the traditional method is also not statistically significant. By visually analyzing the image data, we found that the original images themselves did not have much of non-uniform/poor illumination that blocked the pathology appearance. That possibly explains why the difference among different methods is negligible.

In order to better understand the overall improvement, in the second part of the experiment, fundus images from EyePACS were used. EyePACS has 35,126 retinal images that are graded (by human graders) into five different categories based on DR severity levels. Out of these 35,126 images, 25,810 images are normal, 2443 images are mild non-proliferative DR (NPDR), 5292 images were moderate NPDR, 873 images are severe NPDR, and 708 images are proliferative DR. We aimed to use almost same number of images for each of these categories for this experiment, in order to ensure fair learning for each category by a deep learning model [13]. We performed data augmentation on the proliferative DR images, specifically by rotation (in the range of $-5°$ to $5°$) and flipping, to increase the number of images by

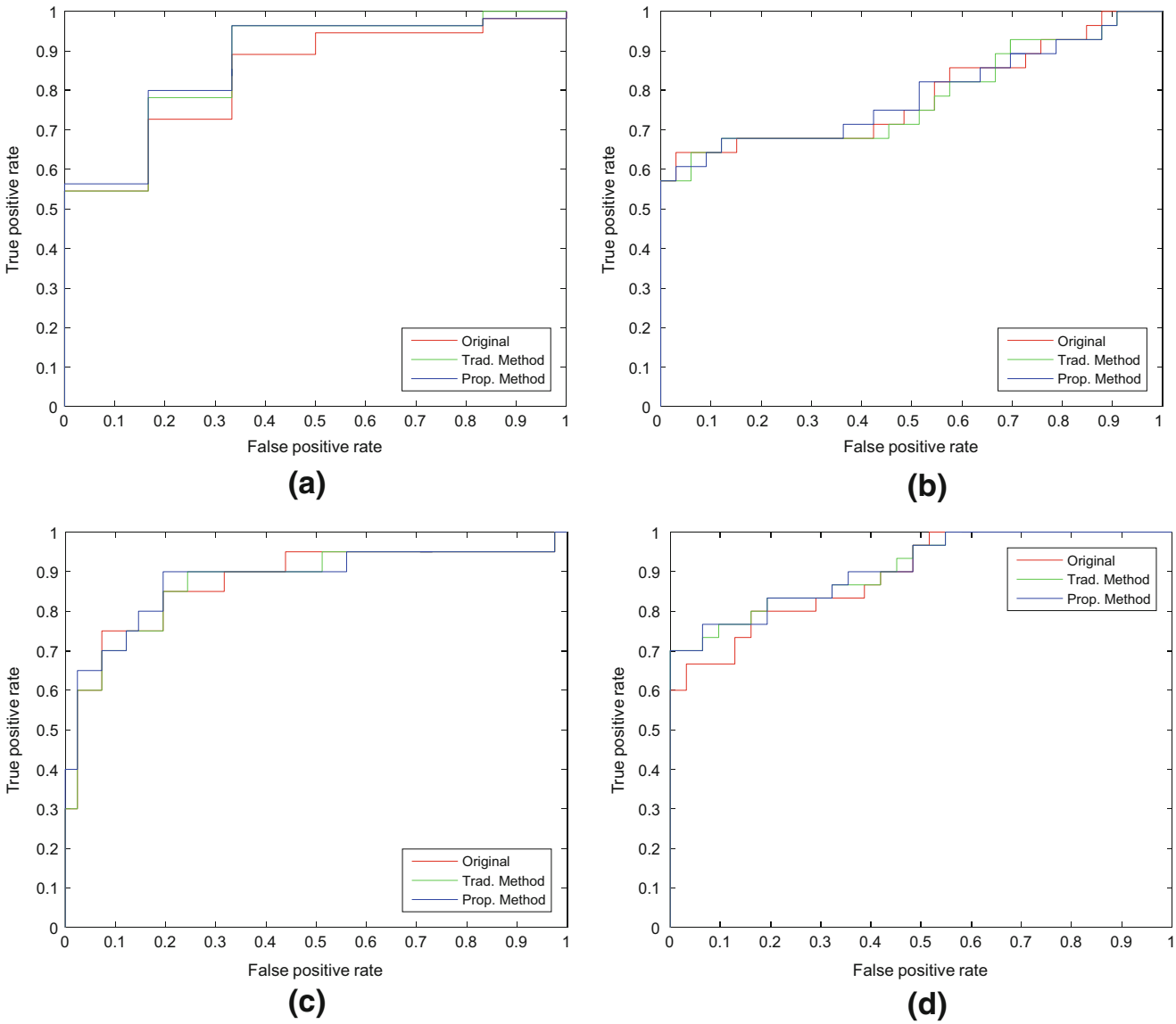

Fig. 6 ROC curves for pathology detection: **a** microaneurysms, **b** hard exudates, **c** soft exudates, and **d** hemorrhages

eight times in this category. Similarly, we performed data augmentation of images in the severe NPDR category to increase their number by six times. For the moderate category, we used all the images. For the mild category, we performed data augmentation likewise to increase the number of images by 2.5 times. For normal images, we selected 6500 images randomly. Thus, for the objective experiment here, a total of 29,664 images were used (details are provided in Table 2).

A deep convolution neural network (CNN) [37] was used to classify the images into five categories as explained above. Specifically, we used the inception v3 model [37] for this experiment. Ninety percent of the data were used for training

Table 1 Area under the ROC curve

Lesion types	Area under the ROC curve (AUC) (in %)		
	Original	Traditional method	Proposed method
Microaneurysms	83.84	86.97	87.37
Hard exudates	78.68	78.58	78.68
Soft exudates	87.56	87.32	88.05
Hemorrhages	89.25	90.86	91.07

Table 2 Details of the image categories used for the experiment

Categories	Number of images
Normal	6500
Mild	6107
Moderate	5292
Severe	6111
Proliferative	5664
Total	29,664

and 10% were used for testing. CNN classifications were performed on the original images and on the illumination-corrected images by the proposed and traditional methods (performed on the HSV space) separately. Without illumination correction, the overall classification accuracy (after 5 epochs) was 56%. With illumination correction by the traditional method, the accuracy turned to 59%, and with illumination correction by the proposed method, the overall classification accuracy turned to 63%.

Discussions and Conclusion

A method for efficient correction of poor and non-uniform illumination of retinal images has been proposed, implemented, and verified. A novel method for estimation of background image in the context of retinal imaging is proposed. Traditional approach applies the smoothing filter directly on the original image to estimate the background, whereas the proposed method splits the background and foreground components and then applies the smoothing filter accordingly. Our subjective and objective experiments have demonstrated that the proposed method performs better than the traditional method and also it does not create false color/artifacts on the image.

Evaluating the performance of the illumination correction method is non-trivial, as suitable metrics are difficult to define [7]. In [9], Varnousfaderani et al. relied on quantitative analysis of retinal features and automated grading using machine learning to evaluate the performance of the proposed correction. While such analysis serves the purpose to some extent, the effect on overall color appearance following correction and creating of false color (if there any) needs further consideration. On that perspective, in line with Kolar et al. [16], we feel that a subjective experiment is necessary along with the objective experiment to properly evaluate a correction method. That is what has been done in this paper.

The subjective experiment confirms that the proposed method does not create false color/artifacts in the image, at the same time performs better illumination correction than the traditional method. In 84 out of 89 cases, the proposed method performs better than the traditional method.

The objective experiment on EyePACS images shows that the proposed method ensures higher accuracy in disease grading than the traditional method when used as a pre-processing technique in a deep learning framework. An improvement of 4% has been observed when illumination correction is performed by the proposed method than the traditional method. For DIRETDB1 dataset, no significant improvement in pathology detection/classification has been observed. However, it is due to the fact that the original images did not have much of non-uniform/poor illumination that could affect pathology detection.

Funding This research did not receive any specific grant from funding agencies in the public, commercial, or not-for-profit sectors.

Compliance with Ethical Standards

Conflict of Interest The authors declare that they have no conflict of interest.

Ethical Approval This article does not contain any studies with human participants or animals performed by any of the authors.

References

1. Jager RD, Mieler WF, Miller JW: Age-related macular degeneration. N Engl J Med 358(24):2606–2617, 2008
2. Cheung N, Mitchell P, Wong TY: Diabetic retinopathy. Lancet 376(9735):124–136, 2010 Available from: http://www.ncbi.nlm.nih.gov/pubmed/20580421
3. Panwar N, Huang P, Lee J, Keane PA, Chuan TS, Richhariya A, Teoh S, Lim TH, Agrawal R: Fundus photography in the 21st century—a review of recent technological advances and their implications for worldwide healthcare. Telemed e-Health 22(3):198–208, 2016
4. Cunha-Vaz J, Rui B, Torcato S, et al: Computer-aided detection of diabetic retinopathy progression. Digital Teleretinal Screening, Berlin Heidelberg: Springer 59–66, 2012
5. Kubecka L, Jan J, Kolar R: Retrospective illumination correction of retinal images. J Biomed Imaging 2010:11, 2010
6. Likar B, Maintz JA, Viergever MA, Pernus F: Retrospective shading correction based on entropy minimization. J Microsc 197(3):285–295, 2000
7. Leahy C, O'Brien A, Dainty C: Illumination correction of retinal images using Laplace interpolation. Appl Opt 51(35):8383–8389, 2012
8. Youssif AAA, Ghalwash AZ, Ghoneim AS: A comparative evaluation of preprocessing methods for automatic detection of retinal anatomy. Proceedings of the Fifth International Conference on Informatics and Systems (INFOS 07) 2430, 2007
9. Varnousfaderani ES, Yousefi S, Belghith A, Goldbaum MH: Luminosity and contrast normalization in color retinal images based on standard reference image. SPIE Medical Imaging, International Society for Optics and Photonics: 97843N–97843N, 2016
10. Foracchia M, Grisan E, Ruggeri A: Luminosity and contrast normalization in retinal images. Med Image Anal 9(3):179–190, 2005
11. Kumari K, Mittal D: Automated drusen detection technique for age-related macular degeneration. J Biomed Eng Med Imaging 2(1):18, 2015
12. Xiao D, Vignarajan J, Lock J, Frost S, Tay-Kearney M, Kanagasingam Y: Retinal image registration and comparison for clinical decision support. Australas Med J 5(9):507, 2012
13. Akram MU, Tariq A, Anjum MA, Javed MY: Automated detection of exudates in colored retinal images for diagnosis of diabetic retinopathy. Appl Opt 51(20):4858–4866, 2012
14. Kande GB, Savithri TS, Subbaiah PV: Automatic detection of microaneurysms and hemorrhages in digital fundus images. J Digit Imaging 23(4):430–437, 2010
15. Grisan E, Giani A, Ceseracciu E, Ruggeri A: Model-based illumination correction in retinal images. 3rd IEEE International Symposium on Biomedical Imaging: Nano to Macro: 984–987, 2006

16. Kolar R, Odstrcilik J, Jan J, Harabis V: Illumination correction and contrast equalization in colour fundus images. 19th European Signal Processing Conference: 298–302, 2011
17. Gonzalez RC, Woods RE: Digital image processing. USA: Pearson Prentice Hall, 2008
18. Russ JC: The image processing handbook, 2nd edition. Boca Raton: IEEE press, 1995
19. Guillemaud R: Uniformity correction with homomorphic filtering on region of interest. Int Conf Image Process 2:872–875, 1998
20. Skifstad K, Jain R: Illumination independent change detection for real world image sequences. Comput Vis Graph Image Process 46(3):387–399, 1989
21. Pham DL, Prince JL: Adaptive fuzzy segmentation of magnetic resonance images. IEEE Trans Med Imaging 18(9):737–752, 1999
22. Vlachos MD, Dermatas ES: Non-uniform illumination correction in infrared images based on a modified fuzzy c-means algorithm. J Biomed Graph Comput 3(1):6, 2012
23. Finlayson G, Hordley S: Improving gamut mapping color constancy. IEEE Trans Image Process 9(10):1774–1783, 2000
24. Jobson DJ, Rahman Z, Woodell GA: Properties and performance of a center/surround retinex. IEEE Trans Image Process 6(3):451–462, 1997
25. Li B, Wang S, Geng Y: Image enhancement based on Retinex and lightness decomposition. 18th IEEE International Conference on Image Processing (ICIP), 3417–3420, 2011
26. Niemann H, Chrastek R, Lausen B, Kubecka L, Jan J, Mardin CY, Michelson G: Towards automated diagnostic evaluation of retina images. Pattern Recognit Image Anal 16(4):671–676, 2006
27. Narasimha-Iyer H, Can A, Roysam B, Stewart V, Tanenbaum HL, Majerovics A, Singh H: Robust detection and classification of longitudinal changes in color retinal fundus images for monitoring diabetic retinopathy. IEEE Trans Biomed Eng 53(6):1084–1098, 2006
28. Zheng Y, Vanderbeek B, Xiao R, Daniel E, Stambolian D, Maguire M, O'Brien J, Gee J: Retrospective illumination correction of retinal fundus images from gradient distribution sparsity. 9th IEEE International Symposium on Biomedical Imaging (ISBI): 972–975, 2012
29. Fairchild MD. Color appearance models, Second Edition, John Wiley & Sons, 2005.
30. Smith AR: Colour gamut transform pairs. ACM Siggraph. Comput Graph 12(3):12–19, 1978
31. Cantrell K et al.: Use of the hue parameter of the hue, saturation, value colour space as a quantitative analytical parameter for bitonal optical sensors. Anal Chem 82(2):531–542, 2009
32. John CR: The image processing handbook, Fifth edition. Boca Raton: CRC Press, 2006
33. Viola P, Jones M: Rapid object detection using a boosted cascade of simple features. Proceedings of the 2001 I.E. Computer Society Conference on Computer Vision and Pattern Recognition (CVPR 2001) 1: I-I, 2001
34. Saha S, Démoulin V: ALOHA: an efficient binary descriptor based on Haar features. IEEE International Conference on Image Processing (ICIP): 2345–2348, 2012
35. Saha SK, Fernando B, Xiao D, Tay-Kearney ML, Kanagasingam Y: Deep learning for automatic detection and classification of microaneurysms, hard and soft exudates, and hemorrhages for diabetic retinopathy diagnosis. Investig Ophthalmol Vis Sci 57(12): 5962–5962, 2016
36. Zhu X, Rangayyan RM: Detection of the optic disc in images of the retina using the Hough transform. 30th Annual International Conference of the IEEE Engineering in Medicine and Biology Society (EMBS 2008): 3546–3549, 2008
37. LeCun Y, Bengio Y, Hinton G: Deep learning. Nature 521(7553): 436–444, 2015